Kufa Journal of Engineering
Vol. 16, No. 1, January 2025, P.P. 421-449
Article history: Received 31 July 2024, last revised 16 October 2024, accepted 8 November 2024

A CRITIC-BPNN APPROACH TO FRICTION STIR WELDING PARAMETRIC SELECTION AND PREDICTION USING AA6082-T6 MATERIAL

Mufutau Adeniyi Abolarin[1], Bayo Yemisi Ogunmola[2], Nehemiah Sabinus Alozie[3], Adeyinka Oluwo[4], John Rajan[5], Swaminathan Jose[6], Sunday Ayoola Oke[7,*], Alexander Iwodi Agada[8], and Ayomide Sunday Ibitoye[9]

[1,2,3,4,7,8,9] Department of Mechanical Engineering, University of Lagos, Lagos, Nigeria

[5] Department of Manufacturing Engineering, School of Mechanical Engineering, Vellore Institute of Technology, Vellore, India

[6] School of Mechanical Engineering, Vellore Institute of Technology, Vellore, India

***Corresponding author: sa_oke@yahoo.com.**

https://doi.org/10.30572/2018/KJE/160123

ABSTRACT

The uncontrolled friction stir welding heat generation impacts the quality of welds. However, the intuition and experience of the engineer fail to regulate the effects of excessive heat generation on the weld quality and research has not addressed this aspect yet. This paper fills the gap by introducing an integrated CRITIC-BPNN (CRiteria Importance Through Intercriteria Correlation-Back Propagation Neural Network) method to investigate the selection and optimisation characteristics of the friction stir welding process for AA6082-T6 material. In this study, two major performance characteristics i.e. ultimate tensile strength (UTS) and percentage elongation (%EL), were chosen for analysis. The input parameters for the machining were the tool rotational speed, welding speed, tool pin profile and tool shoulder diameter. For the back propagation neural network model, a four-layer network with sigmoid hidden neurons and output neurons was selected. The weight estimates of the friction stir welding parameters are determined by the CRITIC method. For further weight determination between the nodes and edges of the neural networks, the Poisson distribution model was introduced. This stochastic-based method was used to calculate the weights at the edges, between the inputs, hidden layers and outputs of the neural network. The forward pass and backward passes are then used for updating and error minimisation. The welding speed has the highest weight with a contribution of 49.72% using the CRITIC method, implying that welding speed is the best and most influential parameter of the friction stir welding process. For the 4-1-2 neural network architecture, the values of the ultimate tensile strength and percentage elongation at the optimal thresholds are 0.6457 and 0.6019, respectively, for the first forward pass and 0.6123 and 0.6356, respectively, for the second forward pass. The predicted tensile strength is 320.64 MPa and the prediction for the percentage elongation is 18.83%. The results obtained from the proposed method could be useful for planning purposes during the friction welding process.

KEYWORDS

Normalization, correlation, tool, a measure of conflict, output weights.

1. INTRODUCTION

In friction stir welding, the prediction and selection of welding process parameters is tedious, requiring a competent evaluation and choice among several alternatives (Sabry et al., 2023; Ay and Sarsilmaz, 2023; Das and Chakraborty, 2024). However, effective multicriteria decision-making strategies that evaluate friction stir welding parameters are scanty, and difficult to rate in importance (Nikolic et al., 2012; Marichamy et al., 2023; Sabry et al. 2023). Hence, there exists the risk of choosing the wrong alternative without scientific support (Das and Chakraborty, 2024). Moreover, multicriteria decision-making has become an important tool to examine information that is unclear, certain and therefore useful to obtain the best decision from limited data in friction stir welding (Marichamy et al., 2023; Sabry et al., 2023; Das and Chakraborty, 2024; Park et al., 2024; Kopf et al., 2024).

Moreover, in friction stir welding, predicting process parameters while utilizing AA6082-T6 material provides valuable information for its stakeholders, including engineers and decision-makers in welding (Kuykendall et al., 2023). Accordingly, artificial intelligence involves several criteria, also implying the appropriateness of introducing multicriteria decision-making methods to solve the current problem is considered (Marichamy and Babu, 2021; Sarvaiya and Singh, 2022). Shaik et al. (2019) enhanced the parameters of joined Al7075-T651 and Al6082-T651 alloys in friction stir welding using the Taguchi GRA (grey relational analysis). Sahu et al. (2021) used FSW on AA5083 to determine the effect of the process parameter on the weld microstructural and physical properties. Sarvaiya et al. (2022) used the PSO (Particle Swarm Optimization) algorithm to attain the best working conditions for the process parameters of FSW and calculated the quality of the performance of FSW under these conditions. Wang and Lados (2022) investigated the friction stir lap welding of two dissimilar galvanized steel sheets (JAC270 45/45 and Al 6061-T651). Gosavi and Jaybhaye (2022) studied the enhancement of the process variables involved in the FSW of the Silicon-Carbon Composite, Al 7075 with the use of Grey Relational analysis (GRA). Gaikwad et al. (2023) estimated various multi-criteria optimisation algorithms for the FSW of AA7075-T651 alloy plates. Akbari and Asiabaraki (2023) evaluated the consequence of the shoulder and probe diameter and height of the FSW tool on the failure load, impact and stress forces and temperature profile of the FS welded AA5083. Dugar et al. (2023) investigated the FSW of AA6082 and AA2014 alloys using Taguchi L9 orthogonal array, analysis of variance and grey relational analysis.

Sefene et al. (2023) utilized a multi-criteria technique to obtain the optimal values of the FSW process parameters that produce welded joints with the best mechanical characteristics. Karthick et al. (2023) analysed the FSW boron and titanium carbide composite of nitinol and estimated its joint's tensile strength using the Taguchi method. Reddy et al. (2023) improved the welding strength when using the Titanium Zirconium Molybdenum tool during the FSW process by using the Taguchi technique. Song et al. (2025) studied the friction stir welded joints of 317L austenitic stainless steel and 2507 super duplex stainless steel, focusing on their surface and mechanical characterization. Abolusoro et al. (2024) studied the joints containing AA7075-T651 and AA6101-TB after being friction stir welded. Tang et al. (2024) analysed the mechanical characteristics and microstructure of a jointed AA6061 material using the friction stir welding method. Xue et al. (2024) established a simulation model to examine the welding process.

Compared with experimental aspects of friction stir welding, little research has been conducted to date on the prediction and selection of metal joint parameters in friction stir welding (Gan et al., 2013; Al-Shaibani and Aljanabi, 2020; Dharmalingam et al., 2022). At the same time, according to cited literature descriptions, the 6XXX aluminum series, including the AA6082-T6 material, has been a major material of interest to researchers and material engineers (Kim et al., 2010; Mallieswaran et al., 2018; Sefene et al., 2023; Rashid et al., 2023; Tang et al., 2024). However, selection and predictive studies are less on the AA6082-T6 material. Recognizing the potential applications of friction stir welded joints of AA6082-T6 material, prediction and selection of parameters in the welding process have been pursued in this work. Moreover, from the literature review and the general understanding of the state-of-the-art in friction stir welding, it is known that the deployment of predictive solutions of the friction stir welded joint parameters and the determination of the best and worst parameters can be considered very promising in the research community and industry. However, no real solutions aimed at predicting friction stir welding parameters for joints, through advanced artificial intelligence applications, fully leveraging the objective multicriteria weight regulation scheme have been proposed and tested in the welding environment. Consequently, no real information associated with the input layer, hidden layer and the overall performance of the artificial neural network intelligent system is available.

Thus, this paper presents an integrated CRITIC-BPNN (CRiteria Importance Through Intercriteria Correlation- Back Propagation Neural Network) method to predict and select metal joint parameters during friction stir welding for the AA6082-T6 material. The CRITIC method is first implemented to determine the objective weights of the neurons in a back propagation network. The mechanisms of forward and backward passes are triggered. Also, the visualization of how to minimize the errors while ensuring that the neural network is reliable is made. The CRITIC method is suggested to sort the parameters and criteria into classes by weights, highlighting the most influential category of the parameters. The back propagation neural network is applied to predict the performance of the metal joint parameters.

The novelty of the work is that a predictive model for the friction stir welding of AA6082-T6 material has been successfully developed using the back propagation neural network. Thus, it reveals the reliability of back propagation neural network method in developing predictive models and making welding decisions towards process sustainability. While the proposed method aided in achieving the highest weld quality level, it is the first investigation within the contemplated parametric range and the proposed method for the AA6082-T6 material, using the friction stir welding process.

The highlights of this study are as follows:

1. The study offers insights into the prediction and selection processes for AA6082 – T6 material friction stir welding and contributes to the development of robust planning of welding practices that align with the economic and environmental objectives of the welding organization.
2. Predicting friction stir welding parameters potentially increases efficiency, reduces operational cost and enhances weld quality.
3. The paper suggests the need for a holistic method that considers the replacement of the common weight used for edges via neural network nodes by including the CRITIC method weight into the back propagation neural network.
4. The Poisson distribution method was used to translate the CRITIC method based weights to those used in calculating the outputs of the hidden layers and the final outputs of the process.
5. CRITIC method enabled the selection of the greatest weight of the friction stir welding parameters for further processing.
6. Analysis of the output for the hidden layer and the final neurons of the neural network using the sigmoid function for activation in the context of friction stir welding of the AA6082-T6 material.

2. METHODOLOGY

2.1. Problem statement

During friction stir welding, excessive heat generation and its poor regulation is a pressing issue that should be addressed. Heat generation, when improperly managed may adversely affect the weld quality of the substrate material being processed. However, attempts at regulating this heat are confronted with multiple challenges such as cost and poor handling of among others. Costs of constructing or purchasing equipment or technology to regulate heat keep escalating day by day, particularly in developing countries whose economies keep on declining by the day. Poorly trained technicians also result in poor handling of the control of heat in the substrate. Moreover, the mechanism of heat generation involves the creation of heat within the friction stir welding process as a result of the dissipation of electromagnetic or electrical energy. Moreover, the prediction of the parameter values of the friction stir welding is a feasible way to overcome the obstacles of cost and poor handling confronting the friction stir welding process. Of great utility in this context is the adoption of the back propagation neural network (Afshari et al., 2016). With very little information on the friction stir welding parameters, an abundant quality of qualitative and quantitative information could be provided for decision-making on heat control in the process. While the traditional back propagation neural network draws its weight from the intuitive experience of the researcher, a new method is needed that ignores the traditional intuitive approach and substitutes it with an objective weight determination multicriteria method. In this context, the CRITIC-based back propagation neural network method may be a suitable candidate to predict the parameters of friction stir welding for the adequate control of heat generation during the welding process.

2.2. Selection of AA6082-T6 material

The AA6082-T6 material has been selected due to its diverse applications in transportation, infrastructure and everyday uses (i.e. firearm suppressors, fly fishing reels, automotive components and non-flight critical aircraft components) (see also Raji and Oke, 2020). The AA6082-T6 material has outstanding properties that make it very attractive to material engineers. These include mechanical properties such as. Brinell hardness of 92, elastic (Young’s tensile) Modulus of 69 GPa, elongation of 9.8%, fatigue strength of 95 MPa, shear modulus of 26GPa and tensile strength of 330MPa. The electrical properties also include an electrical conductivity of 42% IACS. The thermal properties include latent heat of fusion of 410 J/g and thermal conductivity of 160W/m-k.

2.3. CRITIC methodical computation in friction stir welding

In normalizing the parameters of the friction stir welding it has been established that there is a need to identify which of the parameters are beneficial and which are non-beneficial. This is essential to determine the best and worst parameters for the process. Accordingly, the four parameters whose experimental data are considered in the present work are scrutinized for appropriate categorizations. First, the tool's rotational speed was analysed for beneficial or non-beneficial categorization (Sameer and Birru, 2020). As such the researcher searched the literature to understand the effect of tool rotational speed on weld (Sameer and Birru, 2020).

It was found that the higher the tool rotational speed the higher the durability of the aluminum being welded (Sameer and Birru, 2020; Amatullah et al., 2022). Moreover, other information was obtained from the literature, which shows that the higher the tool rotational speed, the higher the quality of the grains produced (Sameer and Birru, 2020). This led the researcher to conclude that the higher the better signal-to-noise criterion is adequate for the tool rotational speed. Hence tool rotational speed is a beneficial parameter (Amatullah et al., 2022). Next is the welding speed. It is found that the higher the welding speed the worse the weld quality will be. Furthermore, with increasing welding speed, the penetration decreases, making the parameters unattractive when increased (Gupta et al., 2019). Thus the lower the better signal-to-noise criterion is applicable and welding speed is non-beneficial. For tool pin profiles, there are various types used such as the square pin, cylindrical pin, tapered pin and trapezoidal pin. It can be concluded that the tool with the square pin gives maximum tensile strength while the tool with the tapered pin profile gives more tensile strength than the cylindrical tool pin (Swetha and Padhy, 2023). This implies that the tool pin is a beneficial parameter in friction stir welding. For tool shoulder diameter, an increase in its value increases the material's mechanical properties. Thus, shoulder diameter is a higher-the-better parameter and hence a beneficial parameter (Sahu and Pal, 2014).

2.4. CRITIC method as a weighted index in the BPNN method

The application of the CRITIC method by the materials engineer is to resolve the complication that arises when confronted with assigning weights to the parameters of the friction stir welding process when they conflict with goals. Here, there are multiple goals to be achieved at the same time. In this context, an objective multicriteria method that assesses uniformly to obtain the same results by different individuals should be used. Specifically, the CRITIC method is used for analysis where the substrate material is AA6082-T6 Fig. 1. Fig. 1 shows the procedural steps observed while executing the CRITIC method. The complete naming of the CRITIC method is the criteria importance through inter-criteria correlation. The procedure utilized in this work entails first the application of the CRITIC method to determine the weights of criteria and then substituting these values in the BPNN (Back propagation neural network) method in the next phase of computation.

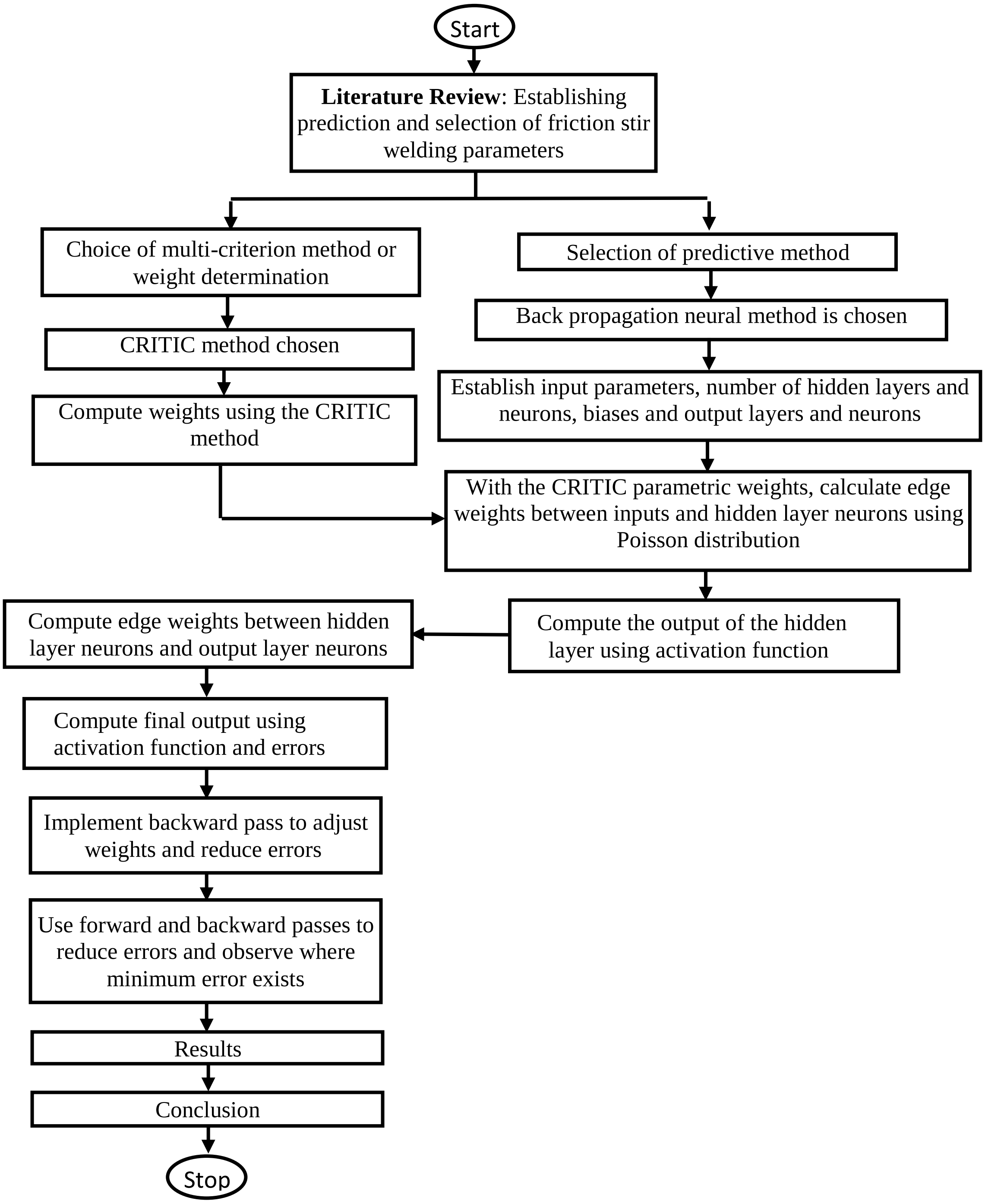

Fig. 1. Research Scheme

Fig. 1 shows the schematic of the proposed method used on the AA6082-T6 material data in the friction stir welding process. It shows first that the idea of the new method was conceived from an understanding of the literature review. Based on the gap revealed in the literature, a predictive model by back propagation neural network was developed. However, it is different from the classical back propagation method because it introduced a mechanism of weight calculation objectively from the CRITIC multicriteria method. So Fig. 1 branches into two parts from the conclusion of the literature review. The first part chooses the CRITIC multicriteria method and the second part selects the back propagation neural network method. After the weights are computed using the CRITIC method on the left side of Fig. 1, the output is fed into the right-hand side of Fig. 1. Here, the inputs are defined, the hidden layers are specified, biases are defined and the outputs are spelt out. Then, the flow of work progresses to the calculation of the weights at the edges. This moves up weight updating in backward passes and the errors are computed. Finally, the results are obtained in back propagation neural networks.

Moreover, the procedure used in implementing the CRITIC method is as follows;

Step 1: Obtain normalized values for all the parameters of the friction stir welding Here, there are four different parameters of interest in the present study namely the tool rotational speed, expressed in revolutions per minute, welding speed, expressed in millimeter per minute, tool pin profile, which has no unit but is expressed in structural form, such as cylindrical, threaded cylindrical, square and trapezoidal. By closely observing the values of the parameters along the four levels defined for each parameter, some values are very high and others are very low. However, it becomes difficult to know which of the very low values of parameters exceed others except by the use of a common analysis, which is called normalization. In the normalization, Equation (1) is used:

$$\overline{X_{ij}} = \frac{X_{ij} - X_j^{worst}}{X_j^{best} - X_j^{worst}} \tag{1}$$

Where $\overline{X_{ij}}$ is the normalized value of the experimental data obtained from Jangra et al. (2015)

X_{ij} is the original value in the non-normalised data

X_j^{worst} is the least or greatest value of a parameter for which assessment is to be made. For a beneficial parameter, it is the least value while it s the greatest value for a non-beneficial parameter

X_j^{best} is the greatest or least value of a parameter for which an assessment is to be made. For a beneficial parameter, it is the greatest value while it s the least value for a non-beneficial parameter

The decision matrix is shown as follows (Adali and Isik, 2017), Equation (2):

$$X = [X_{ij}]_{mxn} = \begin{bmatrix} X_{11} & X_{12} & . & . & . & X_{1n} \\ X_{21} & X_{22} & . & . & . & X_{2n} \\ . & . & . & & & . \\ . & . & & . & & . \\ . & . & & & . & . \\ X_{m1} & X_{m2} & . & . & . & X_{mn} \end{bmatrix} (i = 1,2,...,m;\ j = 1,2,...,n) \tag{2}$$

To applying Equation (1), the parameters are first classified into beneficial and non-beneficial parameters. Beneficial parameters are those elements of the process whose increments are desired and contribute positively to the progress of the friction stir welding process. However, if a parameter contributes negatively to the friction stir welding process whose value increments are not desired then it becomes a non- beneficial criterion. Thus in implementing Equation (1) to the friction stir welding process the maximum value is the best value for beneficial parameters and minimum value is the worst value. For non-beneficial parameters, the minimum value is the best while the maximum value is the worst. Furthermore, the worst value of the parameter is subtracted from the particular value in the cell whose value is to be replaced with the normalized values. This becomes the numerator, which is divided by the difference between the best and the worst values of the parameters. By solving the previously discussed calculation, new values are obtained for each parameter along the levels. Then, computations proceed to the next step.

Step 2: Calculate the standard deviation, σ_j for each parameter (Achebo and Odinikuku, 2015).

For each parameter with the normalized values, the formula for standard deviation is applied on the parameter. This is shown as Equation (3):

$$\sigma_j = \sqrt{\frac{\sum (x_i - \mu)^2}{N}} \tag{3}$$

Where σ_j is the standard deviation of the parameters

N is each value from the parameters

x_i is each value from the parameters

μ is the parameter mean

Using the standard deviation, effort is made to compute the mean of the data values. Afterwards, the deviations of each parametric value from the mean are evaluated. The resulting value is divided by the size of the parameters and the square root of the values are obtained. Then computation proceeds to the next step.

Step 3: Establish the symmetric matrix of nxn with element rjk, which is the linear correlation coefficient between vectors x_j and x_k.

Here a matrix is created which consists of parameters along the x-axis and the same parameters repeated along the y-axis in a matrix.

Then the entries are compared against one another. Now, the linear correlation between parameters is to be calculated. If a parameter is compared against itself, the linear correlation is 1, otherwise it may be less. It should be noted that for both the standard deviation and correlation, the syntax available in Microsoft Excel could be used and it brings results fast. After all the calculations, the symmetric matrix is obtained and the computation proceeds to the next step.

Step 4: Compute the measure of the conflict created by criterion j with respect to the decision situation defined by the rest of the criteria.

Equation (4):

$$M_C = \sum_{k=1}^{m}(1-r_{jk}) \tag{4}$$

Where M_c is the measure of conflict

The values presented from the last step are called the rjk values. However, each of these values needs to be subtracted from 1. Then the sum of each row is evaluated to find the measure of conflict created by the parameter rjk with respect to the decision situation and considering the rest of the parameters. The computation then proceeds to the next step.

Step 5: Establish the quality of the information in relation to each parameter. Equation (5) used in this situation.

$$C_j = \sigma_j \sum_{k=1}^{m}(1-r_{jk}) \tag{5}$$

Where σ_j is the standard deviation of the parameters

What is done in Equation (5) is to multiply the standard deviation value with those of the measure of conflict. On solving, the quality of the information is obtained. The computation afterwards proceeds to the next step.

Step 6: Establish the objective weights:

Here, Equation (6) is used

$$W_j = \frac{C_j}{\sum_{k=1}^{m} C_j} \tag{6}$$

Where W_j is the objective of the parameters

2.5. The BPNN and the CRITIC-based BPNN methods

The BPNN is a state-of-the-art technology with huge flexibility conditions and adaptability, including the CRITIC method, to enhance prediction of the BPNN method. The BPNN is a reliable and highly sophisticated tool used in prediction and decision making. Moreover, with the complex nature of friction stir welding process in view, together with the goal of green welding, a novel BPNN method was developed. The weight estimates of the friction stir welding parameters are determined by the CRITIC method. By using the CRITIC-based weights for initialization and further weight determination between the nodes and edges of the neural networks, the Poisson distribution model was introduced. This stochastic-based method was used to calculate the weights of the edges between the inputs and the hidden layers of the neural network. The Poisson distribution model also aided to determine weights for the edges between the hidden layers and the final outputs. The lambda variable was determined based on some defined properties of the friction stir welding process. The forward pass is then achieved with the computation of weights for the edges and the errors. Weight updating is then implemented and backward pass is used to minimize errors until the error reaches an acceptable threshold.

The following are the principal steps to implement the back propagation neural network applied in this paper:

Step 1: **Forward pass:** In this step, the obtained weights of the parameters through the CRITIC method are fed into the input layer. Afterwards, each input weight is transferred into inputs to be used at the edges by introducing the Poisson distribution function which has three terms namely lambda to the power of X, exponential to the power of negative lambda. These are the numerator of the probabilistic friction while the denominator is the factorial of X. Thus the outcome of the division of the numerator with the denominator is of interest to the analyst for further calculations. In this probabilistic function, to obtain Lambda, the analyst should draw the neural network architecture and analyse each input neuron for Lambda values. The number of edges emerging from each input neuron becomes the denominator value for the Lambda while the particular numbered edge takes the numerator position for the calculation of Lambda. For instance, at the Trs neuron of the input, two edges branch out of it. The label at the first branch edge is W_1, indicating weight at the edge connecting T_{rs} neuron with the first hidden layer labelled Q_1. The second edge branched out to meet the second hidden layer labeled as Q_2. The weight on this edge is W_3. Now, the Lambda value associated with W1 being the first edge is ½ while it is 2/2 for W_3. This same idea is used to generate all the weights, which are conventionally taken as random numbers. However, to obtain X that will be introduced to the Poisson distribution function, we have to refer to the obtained weights by the CRITIC method. Observe that first right after the decimal and take it as the value of X. For instance, the weight obtained for the T_{rs} neuron using CRITIC method was 0.1689. The value X from this number is 1 since it is the first digit after the decimal.

All the edges that enter in Q_1 from the various inputs are multiplied with their corresponding weights and the final value will be added to the bias value, which is randomly generated. The final answer is the value of Q_1. The same procedure will be used for Q_2. Then the actuation function is introduced to calculate the outputs of Q_1 and Q_2. Then the outputs of Q_1 and Q_2 will be those to calculate U_1 and U_2. Then the output of U_1 and U_2 are calculated using the activation function.

Step 2: **Error calculation:** After the output layer has generated the final output, it is compared with the desired output which has been set earlier. This desired output is also called the target output. In the present study, a new innovative approach is developed to represent the target output. The target output is shown as a logarithm function, with a constant added to it, in general it is written as (log f(x)+c)-c. The difference between the target output and the final output is called the total error of the process and is computed to understand how far the total output is from the desired output.

Step 3: **Backward pass:** From the term backward propagation, the backward pass is the most related to this term. However, it is only achieved when a forward pass has been done and error has been calculated. The error value that has been calculated in the previous step is used to evaluate the gradient of the lost function. Then the gradient of the error is transmitted backwards in the entire network. Notice that in forward propagation, the calculation is done from the input to the hidden layers and then the output. However, the reverse is the case with the backward pass, where the output layer is the starting point and information is transmitted to the hidden layers and then to the input. During the propagation of the error backwards, the weight represented by edges is updated in a proportion equal to their contribution to the error. Backward propagation involves obtaining derivatives of the error while each weight is referred to, this shows the extent of change in the weight and how it changes the error. Learning rate is calculated which reveals the size of the weight update. With a small learning rate, the weights are updated in a small manner and vice versa.

Step 4: **Weight updating:** After the derivative of the total error with respect to the weight has been defined, the updating of weight commences using the formula which accounts for the new weight, the current weight, the learning rate and the derivative of the total error with respect to the weight. In the opposite direction of the gradient, the weights are updated and the term gradient descent is often used. A stoppage to weight updating is implemented if the network performance fails to substantially improve.

3. RESULTS AND DISCUSSION

3.1. CRITIC method in friction stirs welding

In implementing step 1 of the CRITIC method, Equation (1) mentioned in the section on methodology is adopted. Table 1 shows the experimental data obtained from Jangra et al. (2015) indicating that there are four parameters of interest in the analysis of this work.

Table 1. Experimental data (Jangra et al., 2015)

Levels	Parameters			
	Tool rotational speed (T_{rs}) rev/min	**Welding speed (S_w) mm/min**	**Tool pin profile (T_{pp})**	**Tool shoulder diameter (T_{sd}) mm**
1	1200	20	1	14
2	1950	25	2	16
3	3080	30	3	18
4	4600	35	4	20
Best	4600	20	4	20
Worst	1200	35	1	14
Delta	3400	15	3	6
Rank	1	2	4	3

The tool rotational speed, measured in revolutions /min, is designated as T_{rs} and classified as a beneficial parameter. The welding speed, measured in mm/min, is represented by letter S_w and regarded as a non-beneficial parameter. The tool pin profile is the third parameter a beneficial parameter represented as T_{pp}, has no units. The fourth parameter, tool shoulder diameter, measured in mm, represented as T_{sd}, is a beneficial parameter. By referring to Equation (1), the researcher is compelled to identify the best and worst parametric values for each parameter. The T_{rs} has its best and worst values as 4600 and 1200 rev/min, respectively. The welding speed, S_w, has its best and worst values as 20 and 35 mm/min, respectively. The tool pin profile (T_{pp}) has its best and worst values as 4 and 1, respectively. Then, the tool shoulder diameter, T_{sd}, has its best and worst diameters as 20 and 14 mm, respectively. With this information, delta values, which are the differences between the highest and lowest in each column (for each parameter) are obtained as 3400, 14, 3 and 6, for T_{rs}, $\underline{S_w}$, T_{pp} and T_{sd}, respectively.

The purpose of Table 2 is to express the values for the parameter in the same scale. Consider the intersection of level 1 and the tool rotational speed, which has a value of 1200 rev/min in Table 1.

Table 2. Normalisation of matrix

Levels	Parameters			
	T_{rs} rev/min	**S_w mm/min**	**T_{pp}**	**T_{sd} mm**
1	0	1	0	0
2	0.2206	0.6667	0.3333	0.3333
3	0.5529	0.3333	0.6667	0.6667
4	1.000	0.0000	1.0000	1.0000
Standard deviation	0.4351	0.4303	0.4303	0.4303

By applying Equation (1), it is known that its numerator has two terms, X_{ij}, which is 1200 and X_i^{worst}, which is still 1200. Then the numerator of Equation (1) is 0. Considering the denominator of Equation (1) which is the difference between X_j best and X_i^{worst}, which is 4600-1200, giving a value of 3400. Then a value of zero divided by 3400 yields 0. The same computation is made for the intersection of level 1 and welding speed to give 1. Other elements along level 1 under the tool pin profile and tool shoulder diameter yield 0 and 0, respectively. Thus, by using the same procedure conducted here for all other levels and parameters, Table 2 is computed with values. Furthermore, along each column representing parameters in Table 2 is the cell after level 4, which should contain the value of the standard deviation. Equation (3) may be used to obtain the standard deviations for parameters. Consider the tool rotational speed having four levels 1, 2, 3 and 4 with normalized values of 0, 0.2206, 0.5529 and 1.0000, respectively. To calculate the standard deviation of the parameters, the mean of these values is first computed as the sum of the values i.e. 0.02206, 0.5529 and 1.0000 divided by 4. This gives 0.4434. However, Equation (3) has the numerator, which demands the subtraction of the mean from each number at the different levels. For instance, at level 1 under tool rotational speed, the indicated value of zero has a value of 0.4434 subtracted from it, which yields -0.4434. Likewise, for level 2 of the same tool rotational speed parameter, 0.4434 is subtracted from 0.226 to give -0.2228. Furthermore, for level 3 of the tool rotational speed parameter, 0.4434 is subtracted from 0.5529 to give 0.1095. Moreover, for level 4 of the tool rotational speed parameter, 0.4434 is subtracted from 1 to yield 0.5566. Notice that the numerator of Equation (3) is summed up after been squared and the square root obtained. In essence, for each of parameters T_{rs}, S_w, T_{pp} and T_{sd}, the standard deviation value obtained are 0.4351, 0.4303, 0.4303 and 0.4303, respectively. Furthermore, Table 3 is created as the correlation matrix which has all four parameters as both its vertical and horizontal axis.

Table 3. Correlation matrix

	Parameters			
Parameters	**T_{rs} rev/min**	**S_w mm/min**	**T_{pp}**	**T_{sd} mm**
T_{rs}	1	-0.9887	0.9886	0.9886
S_w	-0.9887	1	-1	-1
T_{pp}	0.9886	-1	1	1
T_{sd}	0.9886	-1	1	1

Here, the Microsoft Excel spreadsheet facility for correlation could be used and the values in Table 3 are obtained. Next is Table 4 which shows the measure of conflict that utilizes the correlation values for further computations. The final result is in Table 5 which is the weight determination.

Table 4. Measure of conflict

	Parameters				
Parameters	**T_{rs} rev/min**	**S_w mm/min**	**T_{pp}**	**T_{sd} mm**	**Sum**
T_{rs}	0	1.9887	0.0114	0.0114	2.0115
S_w	1.9886	0.0000	2.0000	2.0000	5.9886
T_{pp}	0.0114	2.0000	0.0000	0.0000	2.0114
T_{sd}	0.0114	2.0000	0.0000	0.0000	2.0114

Table 5. Weight determination

Parameters	Standard deviation	Sum	C_j	W_j	W_j (%)
T_{rs}	0.4351	2.0115	0.8752	0.1689	16.89
S_w	0.4303	5.9886	2.5769	0.4972	49.72
T_{pp}	0.4303	2.0114	0.8655	0.1670	16.70
T_{sd}	0.4303	2.0114	0.8655	0.1670	16.70
		Sum	5.183		

All the values of C_j need to be added. Then divide the sum value with each value. On solving, the weights are obtained but have to be expressed in percentage. These are the objective weights of the parameters and can be used in the BPNN method for predictions. Next is the implementation of the BPNN method. For the friction stir welding process, the prediction problem for the parameters is conceptualized as a back propagation method.

3.2. CRITIC based back propagation neural network

In this study, two major performance characteristics i.e. ultimate tensile strength (UTS) and percentage elongation (%EL), were chosen for analysis. The input parameters for the machining were the tool rotational speed (T_{RS}), welding speed (S_W), tool pin profile (T_{PP}) and tool shoulder diameter (T_{SD}). For the back propagation neural network model, a four-layer network with sigmoid hidden neurons and output neurons was selected. Earlier, the CRITIC method was deployed on the experimental data obtained by Jangra et al. (2015) with the result indicating the weight of each of the parameters for T_{rs}, S_W, T_{pp} and T_{sd} the weights are 0.1689, 0.4972, 0.1670 and 0.1670, respectively. These weights are not sufficient for use in the back propagation neural network method because more weights are required than those generated. To overcome this problem, the Poisson distribution is introduced to calculate the weight used at every instance. Consider, the first weight for the tool rotational speed having a value of 0.1689. The value of the parameter with which a factorial is to be obtained is the one after the decimal point, which is 1. Another parameter of the Poisson distribution is Lambda which can be obtained from the number of weight that emerges from the tool rotational speed of concern. This is taken as ½ for the first weight. Thus by applying the Poisson distribution the obtained probability is 0.3033, this weight is assigned to the edge between the mode carrying T_{rs} and Q_1 as in Fig. 2. To obtain the weight of the second edge that connects node T_{rs} and Q_2, which is W_3, a similar procedure is applied such that the Poisson distribution formular is introduced with x maintained as 1. Notice that, this is the value of the whole number after the decimal point of the weight obtained from the analysis by the CRITIC method. Here, Lambda is calculated as 2 since it is the second edge out of a total of two. By substituting these known values into the Poisson equation, W_3 is obtained as 0.0153. By following similar procedure as discussed here and using the obtained weight for S_w, T_{pp} and T_{sd} the estimated weights of the following edges are known: W_2, which is the S_w–Q_1 edge is 0.0016 and for W_6, representing the S_w–Q_2 edge is 0.0153. In addition, W_4, which shows the weight of the T_{pp}–Q_1 edge is 0.3033. Furthermore, W_7 which shows the weight of the T_{pp}- Q_2 edge is 0.3679. Moreover, W_5 which is the weight for the T_{sd}–Q_1 edge is 0.3033. Also, W_8 which is the weight of the T_{sd}–Q_2 edge is 0.3679. Moreover, by considering the neural network architecture in Fig. 2, there are four inputs, namely, T_{rs}, S_W, T_{PP} and T_{sd}. These inputs are linked to the hidden layers Q_1 and Q_2 while they are associated with the biases, b_1 and b_2. Consider the input T_{rs}, it transfers information to the hidden layer Q_1 through weight W_1. The output of the hidden layer Q_1 goes to the output V_1 through the weight of W_{12}. At this output, the information is back propagated into T_{rs} such that the weights are re-evaluated. This procedure, illustrated with T_{rs} is also repeated for each input, namely, S_W, T_{pp} and T_{sd}. The question at this stage, which if answered, will aid the progress of this evaluation, concerns what the output of the hidden layers Q_1 and Q_2 will be. As a computational strategy, an equation is first formulated among the hidden layers, inputs, weights and a bias. A linear equation is assumed among the variables such that the hidden layer becomes the dependent function. While the inputs, weights and bias associated with the first segment of the analysis are the independent functions.

To start with, Equation (7) is formulated:

$$T_{rs}(W_1) + S_W(W_2) + T_{PP}(W_4) + T_{sd}(W_5) + b_1 \tag{7}$$

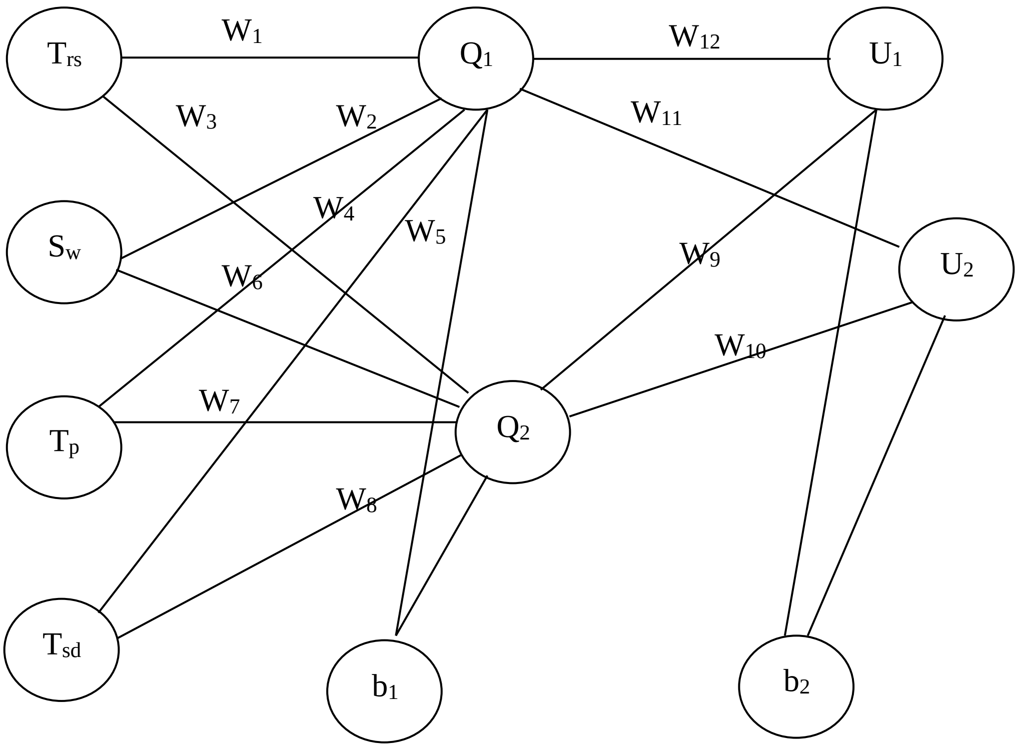

Fig. 2. CRITIC-based BPNN for the friction stir welding process

$$Q_1 = T_{rs}(W_1) + S_W(W_2) + T_{PP}(W_4) + T_{sd}(W_5) + b_1. \quad (8)$$

To obtain Q_1, the various values of the independent variables were introduced into the equations. Here, T_{rs}, S_W, T_{PP} were obtained from the computations of the critic method as 0.1689, 0.4972, 0.1670 and 0.1670 respectively. Furthermore, the computed values of W_1, W_2, W_4 and W_5 are 0.3033, 0.0016, 0.3033 and 0.3033 respectively. However, the value of b_1 needs to be generated randomly as 0.35. All these values of input, weight and bias were substituted into equation 4 to obtain Q_1 as 0.5033. Furthermore, it is in turn to calculate Q_2 and Equation (9) is formulated for this purpose.

$$Q_2 = T_{rs}(W_3) + S_W(W_6) + T_{PP}(W_7) + T_{sd}(W_8) + b_1 \quad (9)$$

From Equation (9), the estimated values of the calculated weights due to T_{rs}, S_W, T_{PP} and T_{sd} are extracted from the critic method as 0.1689, 0.4972, 0.1670 and 0.1670 respectively. In addition, W_3, W_6, W_7, and W_8 are extracted from the calculated weight using Poisson distribution as 0.3679, 0.0153, 0.3679 and 0.3679, respectively. Also, the bias b_1 is 0.35. By substituting all these known values into equation (5), Q_2 is obtained as 0.5426. Output of hidden layer: In this network architecture the hidden layer has members namely Q_1 and Q_2. While each of these layers is fed with inputs from T_{rs}, S_W, T_{PP} and T_{sd}, they get transformed and produce outputs. In essence, there is an output of Q_1 and also an output of Q_2 to be computed. First, the output of Q_1 is estimated using the sigmoid function. This is based on the assumption that the graph evolving from the output of Q_1 as well as Q_2 has a characteristic shape curve. This is a common assumption in artificial neural network and has attracted wide usage in the artificial neural network community. Besides this other researchers utilize other aviation functions such as Tanh, Swish, Relu among others. However, progressing with the use of sigmoid function in evaluating the output of Q_1, Equation (10) is applied.

$$\text{Output of an hidden layer} = \frac{1}{1+e^{-hidden\ layer}} \quad (10)$$

Now, by substituting the value of Q_1 obtained from a previous calculation which is 0.5033 into Equation (10), out Q_1 = 0.6232. Also by substituting the value of Q_2 obtained into Equation (10), Q_2 is obtained as 0.6324. Moreover, moving from the hidden layer to the output of the neural network, elements U_1 and U_2 are considered. Here, equations are formulated to relate U_1 with the output of Q_1, with W_{12}, output of Q_2, with W_9 as well as the bias 2. In this instance Equation (11) is formulated:

$$U_1 = \text{out } Q_1 \times W_{12} + \text{out } Q_2 \times W_9 + b_2 \quad (11)$$

By substituting the appropriate values in Equation (11), U_1 gives 0.6003. Moreover, by evaluating the output of V_1 using a similar approach to Equation (10), out U_1 gives 0.6457. Furthermore, Equation (12) is formulated to relate U_2 as a dependent variable with independent variables such as out Q_1 (W_{11}), out Q_2 (W_1) bias 2. Thus, Equation (11) is expressed as

$$\text{Out } Q_1 (W_{11}) + \text{Out } Q_2 (W_{10}) + b_2 \tag{12}$$

By introducing the appropriate values into Equation (11), U_2 gives 0.6039. Moreover, a similar equation to Equation (10) is used to evaluate the output of U_2, which is obtained as 0.6465.

3.3. Training phase

During the training phase, data on the various parametric values are fed at the input neurons while the final outputs are specified. By observing pairs of neurons the neural network learns by updating its edge weights. This training phase is accomplished by using three principal ideas including back propagation, which is the backward pass conducted after the forward pass that computes the weights. The second idea of the training place is the optimizers while the third content is the loss function. These concepts interact to produce trained neuron that works towards the generation of predicted outputs. Moreover, the neural network parameters are initialized randomly and this is effectively done in the classical literature. However, to diverge from this established practice, in this article, the Poisson distribution is introduced to displace the random weights generation for a methodical evaluation. From the outset, the data on friction stir welding parameters is passed to the network while it generates some probability of the data based % elongation and ultimate tensile of the data.

This prediction together with the actual ground truth of 1 is transmitted to a loss function, which then generates a scalar loss value. Here, the loss function reflects the characteristics of the network. In computations, the weight of the network is adjusted to minimize the loss. However, because of this minimization, calculus is used while the loss propagated to computer gradients. This latter idea is the back propagation of errors. This is because computations are made from the last layer to the second to the last and then up to the first layer in a backward progression. The second idea mentioned above is the optimizers, which behave similarly to gradient descent. The optimizer expresses the parameters as a function of itself, the learning rate and the gradient. The gradient is always calculated during back propagation and it reflects the manner in which the neural network should be updated. Now, on the neural network parameters are calculated, the edge weights are updated. At this stage, the performance of the neural network is judged to be relatively better than the previous performance. The process of forward and backward process is repeated until the error value stabilizes, which is termed the convergence of the results.

3.4 Setting the target for control purposes

Having obtained the outputs U_1 and U_2, it is essential to set target and work backward after achieving a forward pass. It is common to arbitrarily pick values in the literature but a deviation for this was taken in the present study that proposed the use of the logarithm function to set the target in the present paper, U_1 was obtained as 0.6457, while U_2 gives 0.6465. However, to obtain a target for each of these assumed value of roughly 50% of the output is added to each. The same value of 50% is substrate and the final result is used as the target. Thus, to obtain the first target, T_1, the following computation is made: 0.3 is added to 0.6457 while its logarithm is evaluated as log (0.9457) which gives - 0.0242 from this value 0.3 is subtracted to give – 0.2342. Furthermore, to find T_2, the following computations were made: 0.4 is added to 0.6465 while its logarithm is evaluated as log (1.0465) which gives 0.0197. From this value, 0.4 is subtracted to give - 0.3803. It is interesting at this point to find out if there are differences between the calculated outputs (i.e. U_1 and U_2, on one side) and the target values (T_1 and T_2, on the other side). From the analysis U_1 is equal to 0.6457 while T_1 is equal to -0.3242. Here, the difference between these two values of U_1 and T_1 is an error, since the best result would be U_1 to be equal to T_1. Similarly, there is a difference between the values of U_2, which is 0.6465 and T_2, which is -0.3803. This difference is also called an error. Furthermore, for the process, it is interesting to find out what the total errors are. In response to this question, Equation (13) is used to evaluate the total error.

$$E_{total} = \sum \frac{1}{2}(target - output)^2 \tag{13}$$

Recall that there are two aspects of the process investigated, which are the outputs and the targets. The outputs are out U_1 and out U_2 while the targets are T_1 and T_2. Hence, Equation (13) may be re-written to include the mentioned parameters, to give Equation (14).

$$E_{total} = \frac{1}{2}(T_1 - Out\,U_1)^2 + \frac{1}{2}(T_2 - Out\,U_2)^2 \tag{14}$$

The first part of Equation (14) is the first error while the second part is the second error which are represented as E_1 and E_2 respectively. By substituting the known values of T_1, T_2, out U_1 and out U_2 into Equation (14), E_1 could be added to E_2 to give E_{total} as 0.9539. Now, the value of 0.9529 is the error obtained for the process. However, by starting without U_1, there is a need to reduce the error in a backward propagation process, such that the various weights are updated. By looking at Fig. 2, the immediate weight to update is W_{12} in a backward propagation process. Thus, error at W_{12} is obtained by calculating the gradient from the last layer to the second to the last layer and progressively so. In this particular instance, the change in loss as a ratio of the change in parameters is expressed mathematically as Equation (15)

$$\text{Error at } W_{12} = \frac{\partial E_{total}}{\partial W_{12}} \tag{15}$$

However, it is challenging to differentiate Equation (15) from the understanding of Equation (14). In Equation (14), there is no term expressed as W_{12}. This means that Equation (14) cannot be differentiated with respect to W_{12} without making some adjustments. Thus, the right-hand side of Equation (14) is separated as shown in Equation (16).

$$\frac{\partial E_{total}}{\partial W_{12}} = \frac{\partial E_{total}}{\partial Out\, U_1} \times \frac{\partial Out\, U_1}{\partial U_1} \times \frac{\partial U_1}{\partial W_{12}} \tag{16}$$

The adjustment made in Equation (16) is to introduce $\partial Out\, U_1$ and ∂U_1 at both numerator and denominator at the same time. This cancels out and permits progress by way of differentiation of the relevant functions. At this point, each of the three components (i.e. the partial derivatives of a term relevant to the other) has its values extracted and calculated as follows:

For $\frac{\partial E_{total}}{\partial Out\, U_1}$, $E_{total} = \frac{1}{2}(T_1 - Out\, U_1)^2 + \frac{1}{2}(T_2 - Out\, U_2)^2$

$$\frac{\partial E_{total}}{\partial Out\, U_1} = 2 \times \frac{1}{2}(T_1 - Out\, U_1)^{2-1} \times -1 + 0 = -(T_1 - Out\, U_1)$$

The above computation results in -)-0.3242-0.6457)=0.9699.

For $\frac{\partial Out\, U_1}{\partial U_1}$, Out U_1 = $\frac{1}{1+e^{-U_1}}$

$$\frac{\partial Out\, U_1}{\partial U_1} = \text{Out } U_1 \text{ (1- Out } U_1\text{)= 0.6457 (1-0.6457)= 0.2288}$$

For $\frac{\partial U_1}{\partial W_{12}}$

$$\frac{\partial U_1}{\partial W_{12}} = 1 \text{ x Out } Q_1 \text{x } W_{12}^{(1-1)} + 0 + 0 = \frac{\partial U_1}{W_{12}} = \text{Out } Q_1 = 0.6232$$

From the above calculations, the values of $\frac{\partial E_{total}}{\partial Out\, U_1}$, $\frac{\partial Out\, U_1}{\partial U_1}$ and $\frac{\partial U_1}{\partial W_{12}}$ were obtained and substituted into Equation (12) such that 0.9699, 0.2288 and 0.6232 are multiplied to give 0.1383. This implies that to obtain a good value, which is relevant to the target, 0.1383 is the change that should be achieved in W_{12}. This call for an updating of W_{12}. Here, there is a rule that is followed in this neural network training. This rule is stated as in Equation (17).

$$\text{Parameters} = \text{parameters} - \text{learning rate x } \frac{\Delta \ loss}{\Delta \ parameters} \tag{17}$$

Equation (13) is re-written as Equation (18).

$$W_{12} = W_{12} - \eta \times \frac{\partial E_{total}}{\partial W_{12}} \tag{18}$$

where η is the learning rate. Usually the learning rate is assumed as a value between 0 and 1. In this work, a value of 0.5 is used as the learning rate. This is updating W_{12}, and substituting the appropriate values in Equation (15), a value of W_{12} given as - 0.06895 is obtained. Furthermore, by following the same process in updating W_{12}, the updating of W_{11}, W_9 and W_{10} is done particularly finalizing with Equation (18) to obtain W_{11} as – 0.07, W_9 as - 0.07 and W_{10} as – 0.0711. The next step is to update the hidden layers by updating weight W_1, W_2, W_3, W_4, W_5, W_6, W_7, and W_8. After updating, the obtained values are W_1 = 0.3033, W_2 = 0.0016, W_3 = 0.3679, W_4 = 0.3033, W_5 = 0.3033, W_6 = 0.0153, W_7 = 0.3679 and W_8 = 0.3679.

Table 6 shows the old weights used for the first forward propagation and the weights obtained after updating the weights during first backward propagation. Table 6 also shows the value of W_1 to W_{12} In the second forward propagation and the updated weights obtained in the second backward propagation of the architecture 4-2-2. Table 7 shows the different weights obtained in the first and second forward passes. It also shows the different values of updated weights obtained in the first and second backward propagation of the architecture 4-2-2. Table 8 shows the outputs of the hidden layer (Q_1 and Q_2) of the first and second forward passes. It also shows the final outputs (ultimate tensile strength and percentage elongation) obtained after the first and second forward propagation of the architecture 4-2-2. Table 9 shows the output of the hidden layer and final outputs for both the first and second forward passes of the neural architecture 4-1-2.

Table 6. Forward and backward passes for the neural network architecture 4-2-2

Weight	First forward pass	First backward pass	Second forward pass	Second backward pass
W_1	0.3033	0.3033	0.3033	0.3036
W_2	0.0016	0.0016	0.0016	0.0025
W_3	0.3679	0.3679	0.3679	0.3682
W_4	0.3033	0.3033	0.3033	0.3036
W_5	0.3033	0.3033	0.3033	0.3036
W_6	0.0153	0.0153	0.0153	0.0162
W_7	0.3679	0.3679	0.3679	0.3682
W_8	0.3679	0.3679	0.3679	0.3682
W_9	0.0002	-0.07	-0.07	-0.1404

Weight	First forward pass	First backward pass	Second forward pass	Second backward pass
W_{110}	0.0031	-0.0711	-0.0711	-0.1456
W_{11}	0.0031	-0.07	-0.07	-0.1434
W_{12}	0.0002	-0.06895	-0.06895	-0.13825

Table 7. Forward and backward passes for the neural network architecture 4-1-2

Weight	First forward pass	Second forward pass	First backward pass	Second backward pass
W_1	0.3033	0.3033	0.3033	0.3036
W_2	0.0016	0.0016	0.0016	0.0026
W_4	0.3033	0.3033	0.3033	0.3036
W_5	0.3033	0.3033	0.3033	0.3036
W_{11}	0.0031	-0.0701	-0.0701	-0.1434
W_{12}	0.0002	-0.06895	-0.06895	-0.1383

Table 8. Outputs of hidden layers and final neurons for the neural network architecture 4-2-2 (two hidden layers)

	Hidden layers		Final neurons	
Description	Q_1	Q_2	**Ultimate tensile strength (UTS)**	**Percentage elongation (%EL)**
First forward pass	0.6232	0.6324	0.6457	0.6465
Second forward pass	0.6232	0.6324	0.6255	0.6251

Table 9. Outputs of hidden layers and final neurons for the neural network architecture 4-1-2 (only one hidden layer)

	Hidden layers	Final neurons	
Description	Q_1	**Ultimate tensile strength (UTS)**	**Percentage elongation (%EL)**
First forward pass	0.6232	0.6457	0.6019
Second forward pass	0.6232	0.6123	0.6356

The optimal back propagation neural network comprises different architecture. For the first architecture, four neurons are in the input layer, two neurons in the hidden layer and two neurons in the output layer (4-2-2) for the first and second forward passes, the errors are 0.9539 and 0.9564. However, for the second architecture, four neurons are in the input layer, one neuron in the hidden layer and two neurons in the output layer (4-1-2). For the first and second forward passes the errors are 0.9971 and 0.9545. It was noted that increasing the number of hidden neurons of the network from one to two gives the best result of 0.9539 at the first forward pass. Therefore, the computation is truncated after the first iteration. The associated performance characteristics are the ultimate tensile strength and percentage elongation of 0.6457 and 0.6039 respectively. On a scale of 0 to 1 of the experimental data, the following information is useful: obtain the difference between the maximum and minimum value of the ultimate tensile strength, which is (330.150 – 286.900), i.e. 52.24. The value of 0.6457 is multiplied with 52.25 and added to the minimum value of 286.900 to give 320.6378 MPa. Also, to calculate the predicted value for percentage elongation, the difference between the maximum and minimum value, which is (21.6 – 14.6), i.e. 7 is obtained. The value of 0.6039 is multiplied with 7 and added to the minimum value of 14.6 to give 18.83%. Thus, the predicted tensile strength is 320.64 MPa and 18.83% was obtained as the prediction for the percentage elongation.

Table 10. Parametric settings for existing study and the present study

S.No.	Parameters	Ighravwe and Oke (2015)	Current study	Comment
1	No. of inputs	4	4	Same
2	No. of outputs	1	2	Higher number of outputs in the present sudy
3	No. of hidden layers	2	2	Same
4	No. of epoch	2000	2	Current study is simplified
5	No. neurons in hidden layer	8	2	Current study is less complicated

Comparing the neural networks used in applications is an important way for us to position our method regarding the existing knowledge in the literature. Accordingly, we compared the structure of our method with Ighravwe and Oke (2015). In Table 10, there are five main parameters used for comparison. Among these, two of the parameters, namely the number of inputs and the number of hidden layers are the same. However, the remaining three parameters are different. For these different parameters, it was noted that the current study has the advantage of being simple while the literature comparison is very complex regarding the values of the parameters in the serial numbers 2, 4 and 5. It can therefore be concluded that our proposed method competes favourably with the existing literature method.

4. CONCLUSIONS

This article applies a new method called the integrated CRITIC-BPNN method to search for the best operating parameters responsible for the effective control of the FSW process.

The key findings of the present study can be summarized as follows:

1. The welding speed has the highest weight with a contribution of 49.72% using the CRITIC method. However, two parameters, namely tool pin profile and tool shoulder diameter have the respective lowest weight contribution of 16.70% each. This implies that welding speed is the best and most influential parameter of the friction stir welding process according to the results from the CRITIC Method.

2. The values of the ultimate tensile strength and percentage elongation at the optimal thresholds, using the 4-2-2 neural network architecture are 0.6457 and 0.6465, respectively, for

the first forward pass. However, it was 0.6255 and 0.6251, respectively, using the second forward pass.

3. For the 4-1-2 neural network architecture, the values of the ultimate tensile strength and percentage elongation at the optimal thresholds are 0.6457 and 0.6019, respectively, for the first forward pass and 0.6123 and 0.6356, respectively, for the second forward pass.
4. The errors at the first and second forward passes, using two hidden layers (i.e. 4-2-2 neural network architecture) were 0.9539 and 0.9564, respectively. However, for the one hidden layer structure (i.e. 4-1-2) neural network architecture) the errors at the first and second forward passes are 0.9971 and 0.9545, respectively.
5. The predicted tensile strength is 320.64 MPa and the prediction for the percentage elongation is 18.83%.

Briefly, this article contributes to the state-of-the-art of FSW selection and optimization problem, offering a new method to join CRITIC and BPNN for the construction of a robust and reliable method. The problem was solved by developing equations for the various computations such as correlation, normalization and other aspects in CRITIC coupled with the equations for weight determinations in forward and backward passes in the backpropagation neural network implementation process. The CRITIC-BPNN method performed very well concerning solution and convergence when the literature data was used to test the method using tool shoulder diameter, welding speed, tool rotational speed and tool pin profile. Based on the existing problems observed in the implementation of this method, one of the next steps of work should be to develop a simplified spreadsheet method for the last aspect of the back propagation neural networks to aid the weight adjustments. However, the PROMETHEE method may be interesting to use in computations for weight determination.

5. REFERENCES

Abolusoro O.P., Khoathane M.C., Mhike W., Omoniyi P., Kailas S.V., Akinlabi E.T. (2024), Influence of welding parameters and post weld heat treatment on mechanical, microstructures and corrosion behaviour of friction stir welded aluminium alloys, Journal of Materials Research and Technology, 32, 634-648. https://doi.org/10.1016/j.jmrt.2024.07.175.

Achebo J., Odinikuku W. E. (2015), Optimization of gas arc metal welding process parameters using standard deviation (SDV) and multi-objective optimization on the basis of ratio analysis (MOORA), Journal of Minerals and Materials Characterization and Engineering, 3, 298-308. https://doi.org/10.4236/jmmce.2015.34032.

Afshari D., Sedighi M., Karimi M.R. and Barsoum Z. (2016), Prediction of residual stresses in resistance spot weld, Aircraft Engineering and Aerospace Technology, 88(4), 492-497. https://doi.org/10.1108/AEAT-11-2012-0206.

Al-Shaibani I.J. and Aljanabi M.K. (2020), Characteristics of hook and intermixing layer of friction stir spot welding AA5052/C10100 joints reinforced by ZnO nano-particles, Kufa Journal of Engineering, 11(3), 1-15. https://doi.org/10.30572/2018/KJE/110301.

Amatullah M., Jam M., Farooq M. Zargor A.S., Magbool A., Khan N. Z. (2022), Effect of tool rotational speed on friction stir welded aluminum alloys a review, Material Today: Proceedings, 62(1), 245-250. https://doi.org/10.1016/j.matpr. 2022.03.220.

Ay M., Sarsilmaz F. (2023), Optimisation of friction stir welding process parameters using multi –criteria decision making approach, Material Testing, 65(4), 603-615. https://doi.org/10:1515/mt.2022-0432.

Das P.P., Chakraborty S. (2024), In search of the best multi-criteria decision making-particle swarm optimization-based hybrid approach for parametric optimization of friction stir welding processes, OPSEARCH, https:/doi.org/10.1007/S12597-024-00757-1.

Dharmalingam S., Donga A.P., Prajapati C.R., Patel A. D., Babariya P.R. (2022), Material properties and tool selection for friction stir welding: a review, 2022 International Conference on Intelligent controller and computing for Smart Power (ICICCSP) pp. 1-5, https://doi.org/10.1109/ICICCSP53532.2022.9862389

Diakoulaki D., Mavrotas G. and Papayannakis L. (1995), Determining objective weights in multiple criteria problem. The CRITIC method Computers and Operations Research, 22(7), 763-770

Dugar Y., Singh N., Kumar A., Vinayagamurthy G., Shanmuganatan S.P., Manguanth M. (2023), Microstructural studies and parametric optimization of dissimilar friction stir welds, Welding International, 37(4), 206-225, https://doi.org/10.1080/09507116.2023.2211283.

Gan W., Li Z.T., Khurana S. (2013), Tool materials selection for friction stir welding of L80 steel, Science and Technology of Welding and Joining, 12(7), 610-613, https://doi.org/10.1179/1743293 07x2123792.

Gosavi S. V., Jaybhaye M. D. (2022), Friction stir welding process optimization of Al 7075/Si C composites using grey relational analysis, Materials Today: Proceedings, 72(3), 719-723. https://doi.org/10.1016/j.matpr.2022.08.493.

Gupta S.K., Mehrotra S., Raja A.R., Vashista M., Yusufzal M.Z.K. (2019), Effect of welding speed on weld bead geometry and percentage dilution in gas metal arc welding of SS409L, Materials Today: Proceedings, 18(7):5032-5039. https://doi.org/10.1016/j.matpr.2019.0.7.497.

Ighravwe D.E. and Oke S.A. (2015). Machining performance analysis in end milling: Predicting using ANN and a comparative optimisation study of ANN/BB-BC and ANN/PSO, Engineering Journal, 19(5), 121-137.

Jangra K.K., Sharma N., Khanna R., and Matta D. (2015), An experimental investigation and optimization of friction stir welding process for AA6082 T6 (cryogenic treated and untreated) using an integrated approach of Taguchi, grey relational analysis and entropy method, Proceedings of the Institution of Mechanical Engineers Part L Journal of Materials Design and Applications, 230(2), https://doi.org/10.1177/1464420715578182.

Karthick P.A., Reddy G. B., SaravanaKumar M., Reddy B.R., SaikiranK.G, Kannan N. S., Ram S. (2023), Taguchi optimization on friction stir welding of nitinol composite, Materials Today: Proceedings, https://doi.org/10.1016/j.matpr.2023.08.183.

Kim W.K., Goo B.C., Won S.T. (2010), Optimal design of friction stir welding process to improve tensile force of the joint of A6005 extrusion, Materials and Manufacturing Processes, 25(7), 637-643, https://doi.org/10.1080/10426910903365745.

Kopf T., Glück T., Gruber D., Staderini V., Eugui P., Fritze G., Mansouri A., Schnall M., Meyer-Heye P. (2024), Process modeling and control for additive manufacturing of Ti-6Al-4V using plasma arc welding - methodology and experimental validation, Journal of Manufacturing Processes, 126, 12-23. https://doi.org/10.1016/j.jmapro.2024.07.072.

Kuykendall K., Nelson T., Sorensen C. (2023), On the selection of the constitutive laws used in modelling friction stir welding, International Journal of Machines Tools and Manufacture, 74, 74-85, https://doi.org/10.1016/j.machtools.2013.07.004.

Mallieswaran K., Padmanabhan R., Balasubramanian V. (2018), Friction stir welding parameters optimization for tailored welded blank sheets of AA1100 with AA6061 dissimilar alloy using response surface methodology, Advances in Materials and Processing Technologies, 4(1), 142-157, https://doi.org/10.1080/2374068 x. 2017.1410690.

Marichamy M., Babu S. (2021), The selection of optimum process parameters on A319 aluminium alloy in friction stir welding MCDM method, Materials Today: Proceedings, 37(2), 228-231, https://doi.org/10.1016/j.matpr.2020.05.080.

Marichamy M., Chockalingam K. (2023), Process parameters for friction stir welding on A319 aluminum alloy using hybrid technique for order of preference by similarity to an ideal solution and grey relational analysis multi-criteria decision-making method, Proceedings of the Institution of Mechanical Engineers, Part E. Journal of Process Mechanical Engineering, 238(2): 945-953, https://doi-org/10./177/09544089231159990.

Nikolic M., Jovanic D., Cockalo D.Z., Dordevic D., Denisa E. (2012), The selection of the arc welding method by using multicriteria analysis: The TOPSIS method, Metalurgia International, 17(2), 51-56.

Park C., Nam H., Kang N. (2024), Effect of welding current on the mechanical properties of Al 5083 alloy processed using high-current gas metal arc welding, Journal of Advanced Joining Processes, 10, Article 100240. https://doi.org/10.1016/j.jajp.2024.100240.

Raji A.O. and Oke S.A., 2020, Optimization of EDM for AA6061/10%Al2O3 AMMC using Taguchi schemes and analytical hierarchy process for weight determination, Kufa Journal of Engineering, 11(3), 42-61. https://doi.org/10.30572/2018/KJE/110304.

Rashid H. A., Vakili-Tahami F., Saeimi-Sadigh M-A. (2023), Creep lifetime of Al6061-T6 pressurized rotating friction stir welded tube subjected to internal pressure and rotational velocity. Welding and creep lifetime optimization, International Journal of Pressure Vessels and Piping, 202, https://doi.org/10.1016/j.iJPyP.2023.104914.

Reddy Y. A, Reddy M. S., Kumaresan M., Johnson P., Gandhi M. M., Kishore J.S., Subbiah R. (2023), Taguchi optimization of friction stir welding of nitinol alloy, Materials Today: Proceedings, https:doi.org/10.1016/j.matpr.2023.08.185.

Sabry I., Mourad A. H., Alkhedher M., Qazani M. R. C., El-Araby A. (2023), A comparative study of multiple – criteria decision – making methods for selecting the best process parameters for friction stir welded A160L alloy, Welding International, 37(11): 626-642. https://doi.org/10.1080/09507116.2023.2270891.

Sahu M., Paul A., Ganguly S. (2021), Optimization of process parameters of friction stir welded joints of marine grade AA 5083, Materials Today: Proceedings, 44(2), 2957-2962.

Sahu P.K. and Pal S. (2014), Effect of shoulder diameter and plunging depth on mechanical properties and thermal history of friction stir welded magnesium alloy, 5th International and 26th All India Manufacturing Technology and Design Research Conference, AIMTDR 2014, pp. 12-17.

Sameer M.D., Birru A.K. (2020), Selection of friction stir welding tool rotational speed for joining dual phase DP600 steel sheets – an experimental approach, Journal of Adhesion Science and Technology, 35(7), 751-776, https://doi.org/10.1080/01694243.2020.1826789.

Sarvaiya J., Singh D. (2022), Selection of the optimal process parameters in friction stir welding/processing using particle swarm optimization algorithm, Materials Today: Proceedings, 62(2), 896-901, https://doi.org/10.1016/j.matpr.2022.040.06.

Sefene E. M., Tsai Y-H., Jamil M., Jatti Y.S., Mishra A., AsmareTsegaio A., Costa E. (2023), A multi-criterion optimization of mechanical properties and sustainability performance in friction stir welding of 6061-T6 AA, Materials Today Communications, Vol.36, https://doi.org/1016/j.mtcomm.2023.106838.

Shaik B., Good G.H., Prasad B.D. (2019), Investigations and optimization of friction stir welding process to improve microstructures of aluminium alloys, Cogent Engineering, 6(1), https://doi.org/10.1080/23311916.2019.1616373.

Song Q., Han Z., Hu Y., Wang D., Ren Z., Zhou J., Zhang Z., Zhao H. (2025), Investigations on mechanical and surface properties of friction stir welded dissimilar joints of 2507 SDSS and 317L ASS, Tribology International, 201, Article 110226. https://doi.org/10.1016/j.triboint.2024.110226

Swetha S. Padhy C. (2023), Tool pin profiles effect on mechanical properties of friction stir welding of dissimilar aluminum alloys, Materials Today: Proceedings, 92(2), 1092- 1098. https://doi.org/10.1016/j.matpr.2023.05.132.

Tang Y., Li W., Zou Y., Wang W., Xu Y., Vairis A., Çam G. (2024), Effects of tool rotation direction on microstructure and mechanical properties of 6061 aluminum alloy joints by the synergistically double-sided friction stir welding, Journal of Manufacturing Processes, 126, 109-123. https://doi.org/10.1016/j.jmapro.2024.07.067.

Wang X., Lados D.A. (2022), Optimization of aluminum-to-steel friction stir lap welding for the fabrication of high integrity structural components, Journals of Advanced Joining Processes, Vol. 5. https://doi.org/j.jp.2022.100114.

Xue W., Xiao L., Tao T., Huang C., He D., Ren X. (2024), A novel method of lateral tool-tilt for optimizing material flow and temperature distribution in friction stir welding, Materials Today Communications, 40, Article 109962. https://doi.org/10.1016/j.mtcomm.2024.109962.